

Table 1. Electron microprobe analysis and atomic formula on the basis of 12 oxygens for garnet grains from lunar sample 12021,22. The following elements were not detected: Cr, Y, K, and Na.

Chemical analysis		Atomic proportions		
SiO <sub>2</sub>	36.1	Si	2.938	3.000
TiO <sub>2</sub>	0.1	Al	0.052	
Al <sub>2</sub> O <sub>3</sub>	21.4	Al	1.991	1.997
FeO	31.5	Ti	0.006	
MnO	1.2	Fe	2.144	3.033
MgO	0.4	Mn	0.083	
CaO	8.7	Mg	0.048	
		Ca	0.758	
Total	99.4			

duced conditions under which the Apollo 11 rocks crystallized (5) and which are considered to hold true for Apollo 12 rocks (1). Although it was not possible to measure the specific gravity of the grains, the refractive index of 1.81 (determined on the third grain) and the cell edge are in accord (6) with the microprobe analysis recalculated into end-member molecules (7): Alm<sub>70.7</sub>-Gro<sub>25.0</sub>Sp<sub>2.7</sub>Py<sub>1.6</sub>.

Garnet has not so far been observed in contact with other minerals in the rock fragments, owing to its apparent rarity and color resemblance to the paler brown pyroxenes. Nor has it been observed in the thin section. We therefore have no direct evidence about its paragenesis or association. However, the anhedral form of the grains suggests that they occur interstitially rather than as phenocrysts or in vugs.

Garnets are a rare constituent of terrestrial igneous rocks (8) and, among 480 garnet analyses collected by Tröger (9), none is reported to occur in igneous rocks of basaltic composition. Almandine-rich garnets are found as phenocrysts in intermediate to felsic extrusives (8) and in cavities in felsic volcanics (10). It is of interest to note also that, for an almandine-rich garnet, the total almandine plus grossular content (95.7 mole percent) of the lunar garnet exceeds that of any terrestrial garnet reported by Tröger.

The presence of garnet in sample 12021 appears to be somewhat of an enigma. The gross mineral assemblage of this rock—spinel, ilmenite, pyroxenes, plagioclase, cristobalite, tridymite, troilite, native iron and minor pyroxferroite, alkali feldspar, and apatite—is very similar to some of the Apollo 11 crystalline rocks, and yet none of the investigators (see *Science*, 30 January 1970) reported garnet in these samples. Since garnet is obviously a rare mineral in sample 12021, it

seems unlikely that differences in bulk rock composition are important; it would seem, instead, that some particular crystallization condition(s) permitted its formation. From our observations of section 12021,2, it would appear that the conditions under which the Apollo 11 crystalline rocks formed (very low oxygen fugacity and extreme crystal fractionation, with the consequent development of iron-enriched liquids) also hold true for this sample, as does the development of a felsic residuum as the end product. The iron-rich composition, the moderate calcium content, and the extremely low magnesium content, together with the relatively high manganese content for a lunar mineral and the absence of zoning, suggest that the garnet, like pyroxferroite, formed late in the crystallization sequence.

R. J. TRAILL

A. G. PLANT

J. A. V. DOUGLAS

*Geological Survey of Canada,*

*Department of Energy, Mines and*

*Resources, Ottawa, Ontario, Canada*

## References and Notes

1. Lunar Sample Preliminary Examination Team, *Science* **167**, 1325 (1970).
2. Two gray-blue grains, less than 100  $\mu\text{m}$  in size, were also isolated and have been identified as amphibole from the x-ray powder pattern. Further study of this mineral is in progress.
3. CuK $\alpha$ , 57.4-mm radius.
4. Analysis was obtained with a Materials Analysis Company model 400S electron microprobe at 20 kv and 0.03  $\mu\text{a}$  specimen current using a chemically analyzed garnet as standard.
5. M. R. Dence, J. A. V. Douglas, A. G. Plant, R. J. Traill, *Geochim. Cosmochim. Acta Suppl.* **1**, 315 (1970).
6. H. Winchell, *Amer. Mineral.* **43**, 595 (1958).
7. The garnets comprise a group of isomorphous minerals having the general formula X<sub>3</sub>Y<sub>2</sub>(SiO<sub>4</sub>)<sub>3</sub>. Because of extensive atomic substitution, the composition is commonly expressed in terms of proportions of the following end-member molecular compositions:

Almandine (Alm)	Fe <sub>3</sub> Al <sub>2</sub> (SiO <sub>4</sub> ) <sub>3</sub>
Pyrope (Pyr)	Mg <sub>3</sub> Al <sub>2</sub> (SiO <sub>4</sub> ) <sub>3</sub>
Spessartine (Sp)	Mn <sub>3</sub> Al <sub>2</sub> (SiO <sub>4</sub> ) <sub>3</sub>
Grossular (Gro)	Ca <sub>3</sub> Al <sub>2</sub> (SiO <sub>4</sub> ) <sub>3</sub>
Andradite (And)	Ca <sub>3</sub> Fe <sub>2</sub> (SiO <sub>4</sub> ) <sub>3</sub>
Uvarovite (Uv)	Ca <sub>3</sub> Cr <sub>2</sub> (SiO <sub>4</sub> ) <sub>3</sub>
8. L. C. Hsu, *J. Petrol.* **9**, 40 (1968).
9. E. Tröger, *Neues Jahrb. Mineral. Abh.* **93**, 1 (1959).
10. R. L. Oliver, *Geol. Mag.* **93**, 121 (1956).
11. We thank M. Bonardi for measuring the x-ray pattern.

22 June 1970

## Earth's Gravity Field: Relation to Global Tectonics

**Abstract.** *An improved solution for the gravity field shows ocean rises, as well as trench and island arcs, as mass excesses. Ocean basins, areas of recent glaciation, and the Asian portion of the Alpine belt are mass deficiencies. Most features appear interpretable as varying behavior of the lithosphere in response to asthenospheric flow.*

An improved determination of the gravity field from satellite orbits, supplemented by terrestrial gravimetry, has been made by Gaposkin and Lambeck (1). The results are given in the form of spherical harmonic coefficients of the potential complete through the 16th degree, plus a few of higher degree; hence the resolution of the data is about 11°, or 1200 km.

The new gravity field is shown in Fig. 1 in the form of free-air gravity anomalies referred to the figure of hydrostatic equilibrium, an ellipsoid of flattening 1/299.8. Anomalies are preferable to the customary geoid heights because the shorter wavelength variations are not obliterated.

The one great consequence of the improved resolution is to break up the two largest features in the southern oceans that appeared in previous solutions (2). A large area of mild anomaly in the South Pacific is now resolved into two negative areas with a positive area between them; the negative areas

are over basins and the positive area is along the East Pacific Rise. In the area between Africa and Antarctica, a single large positive feature centered in the "vee" between the two rises is now divided into two positive features over the rises and an area of mild anomaly between. Thus the great majority of ocean rises are now seen to be associated with positive anomalies, rather than being of mild anomaly, as inferred from older data. The new solution also shifts or modifies several other features whose correlation with tectonics has previously been puzzling (2).

As in earlier studies, the correlation of gravity with topography is poor for 5th and lower degrees, suggesting a deep-seated cause for this part of the field, such as that recently hypothesized by Hide and Malin (3). The gravity field residual to the 5th degree does, in fact, have significantly higher correlation of positive anomalies with ocean rises. This correlation is even more emphasized if isostatic, instead

of free-air, anomalies are used (see Fig. 2). For example, a large segment of the Pacific-Antarctic Rise, which is negative in Fig. 1, is positive in Fig. 2.

It is appropriate to analyze the gravity field in terms of reasonably contiguous blocks of anomaly  $\times$  area, since, by the half-space application of Gauss's theorem, this quantity is directly proportional to excess mass, which in turn is a measure of the stresses entailed (2). Table 1 gives all such blocks whose anomaly  $\times$  area exceeds  $90 \times 10^6$  mgal  $\times$  km<sup>2</sup>, equivalent to about  $2 \times 10^{21}$  g of mass excess or deficiency.

Although areas of recent glaciation have negative gravity anomalies, their moderate magnitude and rapid rate of uplift emphasize the existence of a rather plastic asthenosphere, with decay times of a few thousand years for broad features (4). All other features must be maintained by asthenospheric flows which, from both theory (5) and observation (6), are essentially steady state; that is, accelerations and decelerations in the Eulerian sense are negligible.

In a steady-state flow system of incompressible material, the maintenance of a mass excess in a particular region can be accomplished by: (i) the piling up of material at the surface; (ii) the replacement of less dense by more dense material at an interior interface; (iii) thermal contraction; (iv) transition to a denser phase; or (v) petrological fractionation in which a less dense component is separated from the material before it enters the region. The reverse of one or more of these processes is required to maintain a mass deficiency. It is to be emphasized that mass transfers are necessary to create mass anomalies; densifications or rarefactions alone are insufficient.

The relationship of gravity anomalies to the flow system depends drastically on the boundary conditions. If the boundary is fixed, a convective upcurrent is associated with a negative anomaly, because of its lower density (7). But if the upper boundary is free (while the lower boundary is fixed), an upcurrent is associated with a positive anomaly because the effect of the mass pushed up at the surface outweighs the density effect (8).

How a boundary behaves between the extremes of perfectly free and perfectly fixed depends on (i) its characteristic decay time in response to a transient loading and (ii) its rigidity and

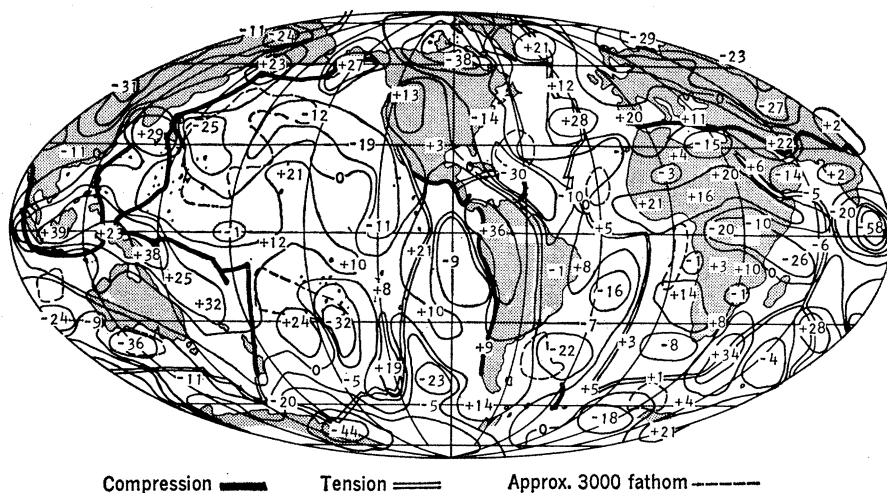


Fig. 1. Free-air anomalies in milligals referred to an ellipsoid of flattening 1/299.8. They are calculated from the spherical harmonic coefficients of the gravitational field of degrees 2 through 16 of Gaposkin and Lambeck (1). (Nonzero contours enclosing only one value have been omitted on all figures.) Global tectonic lines of compression and tension are taken from Isacks *et al.* (9); major basins are indicated by approximate 3000-fathom line.

thickness. The decay time under small stresses of the lithosphere is very long; it is effectively acting as an elastic layer in areas of postglacial uplift. In the major areas of mass excess, the effective decay time may be shorter because of the nonlinear dependence of strain rate on stress, as evidenced by the seismicity of these regions. But for both

the anelastic and elastic behavior, we should expect that the thicker, colder, less hydrous the lithosphere is in a particular region, the more it will behave like a fixed boundary for asthenospheric flows.

Of the major feature types in Table 1, the two of active ocean rise ("rise") and trench and island arc ("arc") are

Table 1. Areas of exceptional gravity anomaly, defined as having an area  $\times$  free-air anomaly (referred to the hydrostatic figure) of more than  $90$  mgal  $\times 10^6$  km<sup>2</sup> ( $2.1 \times 10^{22}$  g) in absolute magnitude and as having absolute anomaly of more than 10 mgal throughout the area.

General location	Area (10 <sup>6</sup> km <sup>2</sup> )	Free-air anomaly $\times$ area (mgal $\times 10^6$ km <sup>2</sup> )	Mean free-air anomaly (mgal)	Type
<i>Positive features</i>				
Sumatra-Philippines-Solomons	18.9	+461.	+27.	Arc
Andes-West Amazon Basin	9.4	206.	22.	Arc-orogenic
Solomons-Tonga-Kermadec	10.4	178.	17.	Arc
Mid-Indian Rise-Indian Antarctic Rise	9.4	175.	19.	Rise
Crozet Plateau-South Madagascar Rise	6.3	117.	19.	Rise
Mexico-Northwest Colombia	7.3	107.	15.	Arc
Carpathians-Turkey-Iran	7.2	103.	14.	Orogenic
Hawaii	6.1	96.	16.	Shield
Azores Plateau	5.8	95.	16.	Rise
Japan-Bonins	4.6	+92.	+20.	Arc
<i>Negative features</i>				
Antarctica	22.4	-511.	-23.	Glaciated basin (?)
Siberian Platform-Turkestan-Himalayas	15.1	289.	19.	Glaciated orogenic
North Canada	10.1	218.	22.	Glaciated
North American-Guiana Basins	11.7	212.	18.	Basin
Somali Basin-Central Indian Ocean	6.2	193.	31.	Basin
North Pacific Basin-Northeast Pacific Slope	12.3	175.	14.	Basin
West Australian Shield-South Australian Basin	4.6	121.	26.	Basin
Northwest Pacific Basin	5.3	116.	22.	Basin
Wharton Basin	5.6	-98.	-17.	Basin

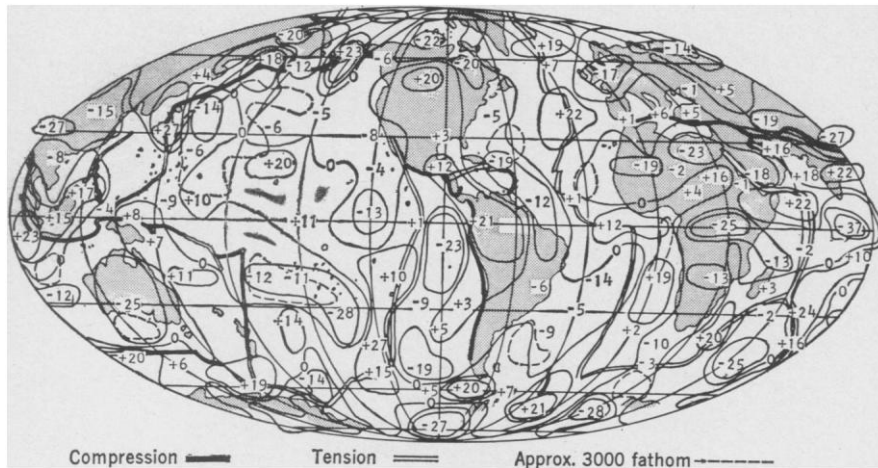


Fig. 2. Isostatic anomalies in milligals referred to a 5th degree spherical harmonic figure. They are calculated from the spherical harmonic coefficients of the gravitational field of degrees 6 through 16 of Gaposhkin and Lambeck (1) and from the coefficients of the Airy-Heiskanen isostatic reduction for a 30-km nominal crustal thickness by Uotila (14).

universally identified as tension and compression zones of the global tectonic system (9). Manifestly, they exhibit differing responses of the lithosphere to convective flow. At the rise the response is closest to that of a free boundary, with several indicators of material weakness: high heat flow, large-scale volcanism, frequent shallow earthquakes, lack of a distinct Mohorovic discontinuity, and so forth. At the arc the response is closer to that of a fixed boundary: the most prominent feature is a colder, denser oceanic lithosphere being thrust down under a less dense but stiffer continental margin, the response being one of resistance to flow possibly from below (10) as well as from above. This resistance implies that the driving force is a push from above rather than withdrawal from below.

The other major compressive feature is the Alpidic belt. The western half, associated with the Mediterranean, appears to have a character similar to the arcs: positive anomalies (marked "orogenic" in Table 1) occur in zones where oceanic lithosphere is being consumed (11). However, the eastern half, associated with the Himalayas-Turkestan complex, has predominantly negative anomalies. A purely continent versus continent compression results in folding rather than downthrust, apparently because of the excessive buoyancy of the thicker crust (12). A mass deficiency occurs at least partly because the stiff lithosphere, containing low density crust, pushes higher density asthenospheric material out of the way; in addition, there may be an astheno-

spheric withdrawal. Glaciation, thermal expansion, and erosion may also contribute to making this area negative. The sedimentation consequent upon erosion is suggested by positive anomalies over the Arabian Sea and Bay of Bengal, which appear in Fig. 2.

The commonest of the major features, the basins of negative anomaly, always occur to the flanks of the rises. The direct source of the negative (on the average, an isostatic anomaly of  $-14$  mgal) is that the crust carried along in the sea-floor spreading is thicker than compatible with the depth of the basin. The problem is the nature of the asthenospheric flow which causes the 3-km drop from the rise to the basin. Either there is an insufficient supply of asthenospheric material in the flow from the rise to match the constant rate of spread of the lithosphere—which means that the asthenosphere is accelerated by being dragged along by the lithosphere—or there is a settling out of a denser component. To constitute a sufficient mass transfer to make the basins isostatically negative, this settling out must occur either between the rise and the basin (possibly associated with the gabbro-to-eclogite phase transition) or at a depth of 300 to 600 km under the basin (possibly associated with the olivine- and pyroxene-to-spinel transition). Mere thermal contraction seems insufficient to induce such a mass transfer. The thick sediments in basins are secondary; if they were the driving force, the isostatic anomalies would be positive rather than negative.

The great negative over Antarctica

also appears to be caused by asthenospheric flow. This anomaly is at least three times too large to be attributable to glaciation (4). Antarctica is about five-sixths surrounded by ocean rises, which are lines of spreading in the global tectonic system. Antarctica lacks the seismicity expected with the destruction or folding of lithosphere. Hence the rises must be moving away from Antarctica. In this case, the Antarctic negative could be caused by an insufficient supply of asthenospheric material in the flow to match the lithospheric rate, as in the first hypothesis suggested for the ocean basin negatives.

Hawaii is unique in being an oceanic positive anomaly far from any rise; it is the only region in the world where the rise-to-continent distance exceeds 5000 km. It appears to require higher temperatures in the asthenosphere that generate excess pressures, together with weaknesses in the lithosphere that allow extrusions. Hawaii may be the site of a partial upcurrent not directly related to the main flow causing the global tectonic pattern—perhaps the reverse of the processes creating the basins.

The achievement of Gaposhkin and Lambeck (1) has been a major improvement in making the gravity field more understandable in relation to other indicators of mantle convection and its interaction with the lithosphere. It is hoped further improvements through new techniques such as satellite radar altimetry and satellite-to-satellite tracking will make gravity data still more valuable in analysis of the earth's tectonics (13).

WILLIAM M. KAULA

University of California,  
Los Angeles 90024

#### References and Notes

1. E. M. Gaposhkin and K. Lambeck, *J. Geophys. Res.*, in press.
2. W. M. Kaula, *ibid.* **74**, 4807 (1969).
3. R. Hide and S. R. C. Malin, *Nature* **225**, 605 (1970).
4. R. J. O'Connell, *Geophys. J. Roy. Astron. Soc.*, in press.
5. D. L. Turcotte and E. R. Oxburgh, *J. Fluid Mech.* **28**, 29 (1967); *J. Geophys. Res.* **74**, 1458 (1969).
6. J. R. Heirtzler, G. O. Dickson, E. M. Herron, W. C. Pitman III, X. Le Pichon, *J. Geophys. Res.* **73**, 2119 (1968).
7. S. K. Runcorn, *Phil. Trans. Roy. Soc. London Ser. A* **258**, 228 (1965).
8. C. L. Pekeris, *Mon. Notic. Roy. Astron. Soc. Geophys. Suppl.* **3**, 343 (1935); D. P. McKenzie, *Geophys. J. Roy. Astron. Soc.* **15**, 457 (1968).
9. X. Le Pichon, *J. Geophys. Res.* **73**, 3661 (1968); B. Isacks, J. Oliver, L. R. Sykes, *ibid.*, p. 5855.
10. B. Isacks and P. Molnar, *Nature* **223**, 1121 (1969).

11. D. P. McKenzie, *ibid.* **226**, 239 (1970).
12. ———, *Geophys. J. Roy. Astron. Soc.* **18**, 1 (1969).
13. W. M. Kaula, *Trans. Instrum. Soc. Amer.*, in press.
14. U. H. Uotila, *Ohio State Univ. Dept. Geodetic Sci. Tech. Rept.* **37** (1962).
15. I thank E. M. Gaposhkin and Kurt Lambeck for providing their results in advance of pub-

lication. This report is drawn from a more extended study to be published in *The Nature of the Solid Earth*, E. C. Robertson, Ed. (McGraw-Hill, New York, in press). This work has been supported by NSF grant GA-10963. Publication 840, Institute of Geophysics and Planetary Physics, University of California, Los Angeles.

11 May 1970

port on laboratory studies with the fungal isolate *Penicillium simplicissimum* (Oudemans) Thom, strain WB-28, which solubilized significant quantities of the Si, Al, Fe, and Mg in several examples of igneous and metamorphic rocks and caused changes in the infrared absorption spectra of some of the residual rock material.

*Penicillium simplicissimum* WB-28 was grown in triplicate in 50 ml of Pope and Skerman's basal mineral salts solution (3) supplemented with 4 percent glucose and 0.01 percent yeast extract in the presence of 500 mg of powdered sterilized rock (4). Three sets of triplicate controls consisted of sterile medium with rock, inoculated medium without rock, and sterile medium. Incubation was in 250-ml plastic Erlenmeyer flasks at 30°C for 7 days on a rotary shaker (2.5 cm excursion diameter, 320 rev/min). After incubation the contents of all flasks were brought to 100 ml with distilled water and centrifuged in plastic ware to remove the mixture of mycelium and residual rock. The supernatant was filtered through Whatman No. 42 filter paper, followed by filtration through a 0.20- $\mu$ m membrane filter (Gelman Metrical GA-8) into plastic bottles. This solution was then analyzed for soluble Si, Al, Fe, and Mg by atomic absorption. The mixture of residual

## Fungal Attack on Rock: Solubilization and Altered Infrared Spectra

**Abstract.** *Penicillium simplicissimum*, isolated from weathering basalt, produced citric acid when grown in a glucose-mineral salts medium with basalt, granite, granodiorite, rhyolite, andesite, peridotite, dunite, or quartzite. After 7 days' growth as much as 31 percent of the silicon, 11 percent of the aluminum, 64 percent of the iron, and 59 percent of the magnesium in some of the rocks were solubilized, and a number of rocks showed altered infrared absorption in the silicon-oxygen vibration region.

The discovery of fossil microorganisms in ancient sedimentary rocks (1) lends strong support to the contention that life has been present on Earth for several billion years. It seems reasonable to expect that during this time at least some microorganisms developed the ability to attack the rocks and minerals of the biosphere, since these substances are the ultimate source of the inorganic elements and compounds required for life. Although participation of microorganisms in the weathering of rocks and minerals has long been ac-

knowledged, very little is known of the specific mechanisms; only a few recent studies (2) have been concerned with this problem. As part of our studies on life detection methods we are investigating the possibility that microorganisms, independent of their fossil remains, might leave a record of their metabolic activity in alterations of the rocks and minerals of their environment.

We screened a variety of microorganisms isolated from the surface of weathering basalt for rapid solubilization of unweathered rock. We now re-

Table 1. Solubilization of the Si, Al, Fe, and Mg of rocks by *Penicillium simplicissimum* after 7 days' incubation at 30°C. Data for the soluble elements in uninoculated controls (in parentheses) and inoculated flasks are the means of triplicate cultures corrected for the elements originally present in the growth medium. Abbreviation: N.D., not determined; < indicates a value below the detection limit given.

Sample	Rock analysis (milligrams per 100 mg of rock)				Soluble rock elements (milligrams per 100 mg of rock)							
	Si	Al	Fe	Mg	Si	Al	Fe	Mg	Si	Al	Fe	Mg
Dunite												
DTS-1	18.97	0.16	6.07	30.07	(0.13)	5.94	(< 0.01)	0.01	(< 0.09)	2.09	(0.18)	8.46
Peridotite												
PCC-1	19.61	.41	5.74	26.15	(.17)	2.86	(< .01)	.04	(< .09)	1.92	(.16)	11.38
Basalt												
D-100043	21.81	7.89	9.70	5.32	(.28)	1.21	(< .02)	.30	(< .03)	2.54	(.02)	2.21
BCR-1	25.30	7.25	9.32	2.09	(.06)	0.33	(< .02)	.15	(< .03)	1.19	(.04)	0.24
A	24.13	8.36	6.23	3.62	(.06)	.59	(< .02)	.58	(< .03)	3.06	(.04)	2.04
Andesite												
AGV-1	27.59	9.05	4.65	0.91	(.06)	.28	(< .03)	.18	(< .07)	0.35	(< .01)	0.08
Granodiorite												
GSP-1	31.44	8.13	2.97	.59	(.04)	.60	(< .03)	.63	(< .09)	1.29	(< .01)	.35
Granite												
G-2	32.36	8.16	1.86	.46	(.05)	.56	(< .03)	.41	(< .01)	0.94	(.01)	.26
D-100429	34.68	6.77	1.63	.05	(.02)	.44	(< .03)	.30	(< .01)	.91	(.01)	< .01
D-100643	35.04	6.63	1.57	.04	(.01)	.47	(< .03)	.26	(< .01)	1.01	(.01)	.01
D-100018	35.36	6.86	0.61	.16	(.02)	.18	(< .03)	.22	(< .01)	0.14	(.02)	.03
D-100012	35.58	7.22	.29	0.00	(.02)	.09	(< .03)	.12	(< .01)	.04	(N.D.)	N.D.
Rhyolite												
D-100051	35.65	6.79	.78	.07	(.04)	.25	(< .02)	.20	(< .01)	.10	(< 0.01)	0.03
D-100050	35.18	7.17	.60	.04	(.03)	.09	(< .02)	.05	(< .01)	.01	(< .01)	.01
Quartzite												
D-100314	34.24	6.24	2.88	1.17	(.02)	.89	(< .02)	.69	(< .04)	1.05	(< .01)	.49
D-100316	37.14	5.09	2.76	0.69	(.02)	.86	(< .02)	.60	(< .04)	0.98	(< .01)	.36